

# Size Effects on the Stabilization of Ultrafine Zirconia Nanoparticles

J. Ch. Valmalette\* and M. Isa

Laboratoire Matériaux Microélectronique de Provence (L2MP), CNRS, UMR 6137,  
Université de Toulon-Var B.P. 132, F-83957 La Garde Cedex, France

Received June 14, 2002. Revised Manuscript Received September 20, 2002

The spontaneous oxidation of crystallized ZrAu at room temperature leads to the formation of ultrafine monoclinic zirconia (MZ) particles (about 3.6 nm in diameter). The presence of tetragonal phase (TZ), generally observed in very small zirconia particles, was investigated by X-ray diffraction and Raman experiments but was not observed. Thermodynamical calculations considering the finite size effects in zirconia were introduced to explain the formation of pure MZ considering experimental and theoretical surface energies. The results of these calculations associated with the near equilibrium conditions used for synthesis demonstrate that the monoclinic structure is the stable crystallographic structure of zirconia nanocrystals at room temperature.

## Introduction

The stabilization of crystallographic phases in solids is strongly influenced by the dimension of particles. The “high-temperature” or high-symmetry phase is generally observed with decreasing sizes and this dependence is commonly described with thermodynamic models derived from the Gibbs–Thomson equation, considering grain sizes and surface effects. The predicted monotonic reduction of  $T_c$  with size can lead for some compounds to a critical grain size for which the “low-temperature” phase does not exist. For example, the thermal phase transition is not at all observed in nanoparticles of displacive systems with a size below  $\approx 25$  nm. Ayyub et al.<sup>1</sup> showed that ferroelectric order in PbTiO<sub>3</sub> powder cannot be sustained below the critical size of 7 nm for which the lattice ratio  $c/a$  is equal to 1.

The stabilization of tetragonal zirconia (TZ) with decreasing particle size has been extensively studied.<sup>2</sup> The various conditions reported in previous works are precipitation in aqueous solution, spray pyrolysis,<sup>3</sup> inert gas condensation,<sup>4</sup> and corrosion of zirconium under water-pressurized reactors. According to several authors, monoclinic zirconia (MZ) cannot be sustained at room temperature below critical sizes of about 15–20 nm.<sup>5</sup> These values are in close agreement with calculations from the contribution of the surface energy proposed by Garvie,<sup>6</sup> which is considered to influence the stability of TZ particles. The pressure dependence of  $T_c$  was described by Whitney<sup>7</sup> in 1965 and completed more

recently by the Raman technique.<sup>8</sup> The size dependence of  $T_c$  is described as monotonic, and Molodetsky et al.<sup>9</sup> even suggested the presence of cubic zirconia particles in powder obtained by calcination of amorphous zirconia. Nevertheless, recent works have also shown that the conditions under which the powder was prepared could considerably modify the range of TZ stability. In 1984 Morgan<sup>10</sup> reported the synthesis of 6-nm MZ particles by hydrothermal treatment; in contrast, Mitsuhashi et al.<sup>11</sup> stabilized 200-nm TZ monocrystals by microwave heating of zirconyl chloride solutions. The morphology of TZ nanoparticles also influences their stability<sup>12</sup> and Srinivasan et al.<sup>13</sup> have shown that  $\approx 10$ -nm TZ particles obtained by precipitation and calcination are partially converted into MZ nanoparticles without crystal growth by annealing at 800 °C. These results have raised doubts about the existence of a critical size for MZ or TZ stabilization.<sup>14,15</sup> The more general mechanism of stabilization or destabilization of crystallographic phases is under discussion and is of considerable interest for predicting nanoscale properties.

In the present work, we describe the preparation of ultrafine zirconia nanoparticles (of about 3.5 nm) by spontaneous oxidation at room temperature of crystallized ZrAu.<sup>16</sup> Under these near equilibrium conditions,

(8) Bouvier, P.; Djurado, E.; Lucaleau, G.; Le Bihan, T. *Phys. Rev. B* **2000**, 62 (13), 8731.

(9) Molodetsky, I.; Navrotsky, A.; Paskowitz, M.; Leppert, V. J.; Risbud, S. H. *J. Non-Cryst. Solids* **2000**, 262, 106.

(10) Morgan, P. E. D. *J. Am. Ceram. Soc.* **1984**, 67 (10), C204.

(11) Mitsuhashi, T.; Ichihara, M.; Fim, C. H. *J. Am. Ceram. Soc.* **1973**, 47 (12), 622.

(12) Shukla, S.; Seal, S.; Vij, R.; Bandyopadhyay, S.; Rahman, Z. *Nano Lett.*, in press.

(13) Srinivasan, R.; Hubbard, C. R.; Burl Cavin, O.; Davis, B. H. *Chem. Mater.* **1993**, 5, 27.

(14) Bernstein, E.; Blanchin, M. G.; Ravelle-Chapuis, R.; Rodriguez-Carvaljal, J. *J. Mater. Sci.* **1992**, 27, 6519.

(15) Hu, M. Z. C.; Hunt, R. D.; Payzant, E. A.; Hubbard, C. R. J. *J. Am. Ceram. Soc.* **1999**, 82, 2313.

(16) Valmalette, J. C.; Isa, M.; Passard, M.; Lomello-Tafin, M. *Chem. Mater.* **2002**, 14, 2048.

\* To whom correspondence should be addressed. E-mail: valmalette@univ-tln.fr.

(1) Ayyub, P.; Chattopadhyay, S.; Sheshadri, K.; Lahiri, R. *Nanostruct. Mater.* **1999**, 12, 713.

(2) Lawson, S. *J. Eur. Ceram. Soc.* **1995**, 15, 485.

(3) Djurado, E.; Meunier, E. *J. Solid State Chem.* **1998**, 141, 191.

(4) Skandan, G. *Nanostruct. Mater.* **1995**, 5 (2), 111.

(5) Chrsaka, T.; King, A. H.; Berndt, C. C. *Mater. Sci. Eng. A* **2000**, 286, 169.

(6) Garvie, R. C. *J. Phys. Chem.* **1965**, 69, 1238.

(7) Whitney, E. D. *J. Electrochem. Soc.* **1965**, 112, 91.

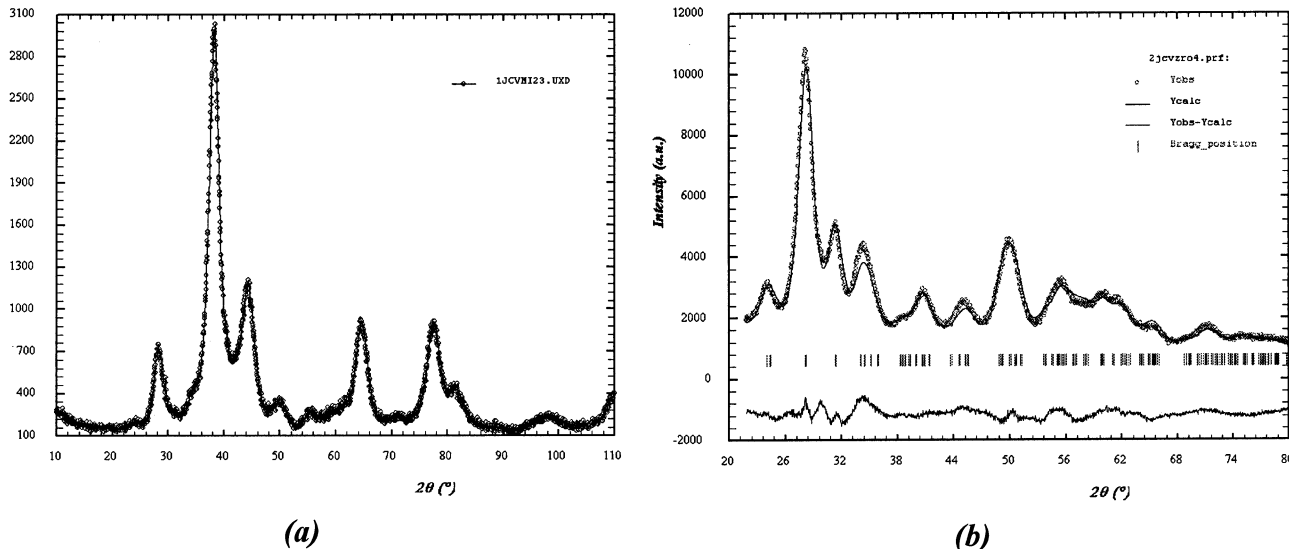
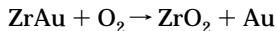


**Figure 1.** X-ray diffractogram of (a) as-prepared mixed powder and (b) washed zirconia obtained by nanostructuring oxidation of ZrAu at 25 °C and Rietveld refinement.

only MZ nanoparticles are formed, as is observed in bulk zirconia. Our experimental results show that size dependence of  $T_c$  is not necessarily monotonic and additional effects could become predominant in very small clusters.

### Experimental Section

Zirconia powder was prepared from the selective oxidation of crystallized ZrAu ingots by the following reaction,



occurring spontaneously in an air laboratory and at room temperature. The unexpected reactivity of the ZrAu compound was discovered recently and described in detail in a previous paper.<sup>16</sup> The products are both nanosized and in powder form. This reaction is very rapid and closely related to the  $P(\text{H}_2\text{O})/P(\text{O}_2)$  ratio. Reactivity decreases drastically in a pure  $\text{O}_2(\text{g})$  atmosphere. The rate of reaction, expressed in terms of transformed thickness on the surface of the alloy, is constant and comprised between 1 and 4  $\mu\text{m}/\text{day}$  under 60% relative humidity at 25 °C. These discrepancies are strongly related to the microstructure of the initial ZrAu.

The mixed powder obtained spontaneously from ZrAu slices ( $1 \times 1 \times 0.2 \text{ cm}$ ) after 1 month was washed in aqua regia to remove gold clusters, rinsed with pure distilled water, and dried in air. The powder is white and can be easily dispersed in suspension. Structural investigations were carried out, on the as-prepared mixed powder and on the washed zirconia, by an X-ray diffraction technique on a Siemens-Bruker D5000 diffractometer using  $\text{Cu K}\alpha$  radiation (35 mA, 45 kV) with a back monochromator over a  $2\theta$  range of 5°–120° and a position-sensitive detector using a step of 0.04°. The mean crystallite sizes were calculated by Rietveld refinements. The FT-IR spectroscopy measurements were carried out with a Mattson-Nicolet RS spectrometer in transmission mode in the 400–4000- $\text{cm}^{-1}$  spectral range by the classic KBr pellet technique. The Raman spectra were obtained using an XY Dilor multichannel spectrometer equipped with a CCD detector. Radiation of the 514.53-nm line from an argon ion laser was used as the excitation source.

### Results

The X-ray diffractogram of the as-prepared mixed nanopowder (Figure 1a) shows intense broad peaks clearly related to fcc gold particles and modulation in

the background corresponding to the reflections of zirconia. The determination of the relative contribution of monoclinic zirconia (MZ) and tetragonal zirconia (TZ) in this powder is uncertain, due to the considerable broadening and overlapping of Bragg reflections. However, Rietveld refinement made on these samples clearly evidenced the presence of MZ associated with the (111) reflection at 28.2°. The determination of particle size was deduced from Rietveld refinement considering Gaussian and Lorentzian contributions.

The overall broadening effects, arising from the small coherent grain size and atomic level strain, were considered. The gold and zirconia particle sizes are respectively equal to  $2.9 \pm 0.2$  and  $3.6 \pm 0.3 \text{ nm}$ .

The X-ray diffractogram of the washed nanopowder (Figure 1b) does not show gold reflections. The modulations associated with zirconia are amplified but not significantly modified by the treatment of the powder. The whole pattern fitting with the additional contribution of TZ was investigated but refinement residues are not significantly improved. The presence of very small MZ particles is apparently in contradiction with the room-temperature stabilization of TZ commonly observed for small particles (smaller than 15–18 nm). The influence of crystal growth induced by thermal treatment up to 823 K was also studied by X-ray diffraction. Analyses made at room temperature show particle growth up to 8 nm (Figure 2) but no changes in diffraction pattern except the narrowing of the Bragg reflection.

Further experiments were made to investigate the presence of small amounts of TZ. Infrared spectroscopy spectra confirm the presence of MZ associated with the characteristic vibrational band at 737  $\text{cm}^{-1}$  but the presence of TZ cannot be evidenced by this technique.

Raman spectroscopy is one of the most sensitive techniques generally used to investigate the structure of zirconia. Samples were analyzed with precaution to avoid a possible phase transition that could be induced by the laser beam. Experiments were made with increasing power from 0.1 to 10 mW with a laser spot of about 2  $\mu\text{m}$  but did not show any thermal effect, except

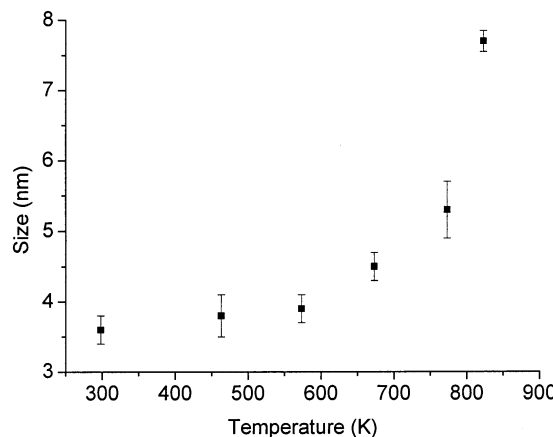


**Figure 2.** Evolution of particle sizes of zirconia upon annealing in air.

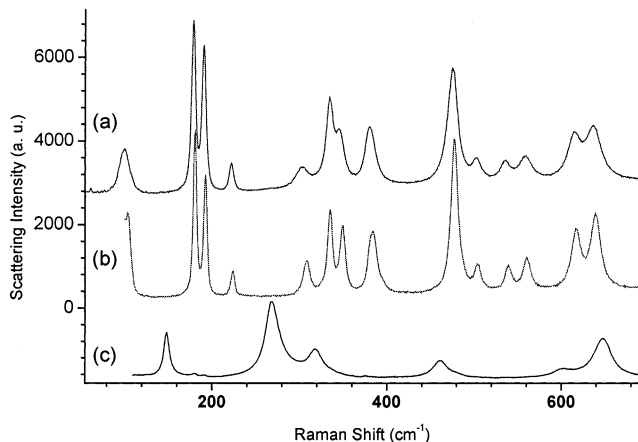


**Figure 3.** Raman spectra of 3.6-nm zirconia obtained by nanostructuring oxidation of ZrAu at 25 °C (a), commercial monoclinic zirconia (MZ) from Tosho (b), and commercial tetragonal zirconia (TZ) from Tosho (c).

for a small and irreversible decrease of the fluorescence. The Raman spectrum presented in Figure 3 shows lines at 100, 191, 304, 345, 475, 559, and 636  $\text{cm}^{-1}$  and 222, 335, 380, 502, 536, and 616  $\text{cm}^{-1}$ , which can respectively be assigned to  $\text{A}_\text{g}$  and  $\text{B}_\text{g}$  modes of MZ. On the other hand, the characteristic lines of TZ are not observable.

The thermal stability of the ultrafine zirconia powder was also investigated by Raman spectroscopy up to 823 K under air. Spectra obtained under these conditions indicate neither a change in symmetry of zirconia nor additional lines.

Therefore, Raman analyses confirm the observation made by X-ray diffraction technique: only ultrafine MZ particles are formed during this process at room temperature, and the monoclinic structure is stable with increasing temperature and particle growth.

## Discussion

The formation of amorphous zirconia (AZ) was not observed during the oxidation of ZrAu at room temperature. This observation confirms the strongly negative enthalpy of transition amorphous zirconia  $\rightarrow$  MZ determined recently by Molodetsky et al.<sup>9</sup> to be about  $-60 \text{ kJ}\cdot\text{mol}^{-1}$  at 298 K. The stabilization of the high-temperature tetragonal polymorph is generally discussed as the result of the combination of temperature,

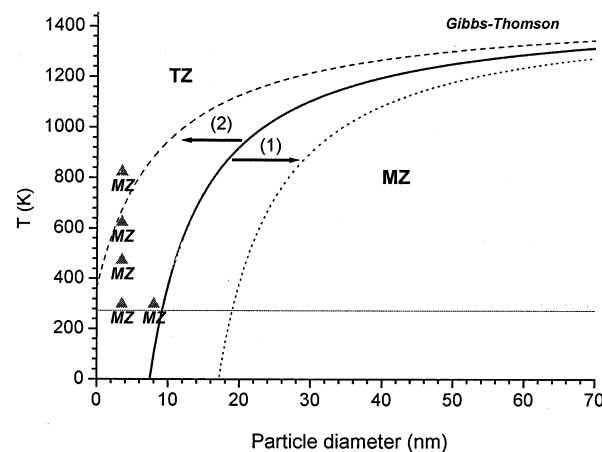


**Figure 4.** Schematic representation of the phase diagram of zirconia in the plane ( $T, r$ ): size dependence of  $T_c$  calculated from the Gibbs–Thomson relation (continuous line), qualitative upshift observed under high pressure (dotted line), downshift under tensile stress (dashed line), and Raman and XRD observations made on ultrafine zirconia particles (noted “ $\Delta$ ”).

pressure, and grain size effects during the formation. The generally agreed phase diagram of zirconia is schematically represented in the plane ( $T, r$ ) in Figure 4. The continuous line corresponds to equilibrium calculated from the Gibbs–Thomson relation initially introduced to describe the size dependence of the melting temperature. The difference  $\gamma_{\text{HT}} - \gamma_{\text{LT}}$  in surface tension was described by Garvie<sup>6</sup> as a key factor of the downshift of  $T_c$ . According to this concept, the higher surface energy of the HT phase counterbalances its lower energy in enthalpy under a critical radius  $r_c$  that we can write as

$$r_c = \frac{-3(\gamma_{\text{HT}} - \gamma_{\text{LT}})}{\Delta H_{\text{tr}} \left(1 - \frac{T_c}{T_\infty}\right)} \quad (1)$$

where  $T_\infty$  represents the transition temperature of an infinite crystal and  $\Delta H_{\text{tr}}$  the enthalpy of transition (expressed in  $\text{J}\cdot\text{m}^{-3}$ ).

Our experimental data obtained by X-ray diffraction and Raman experiments on ultrafine zirconia particles at different temperatures and for different sizes are reported in Figure 4 (noted “ $\Delta MZ$ ”) and are in contradiction with simulations based on the Gibbs–Thomson relation. The structural stability of these small MZ particles is evidenced within a wide temperature range (298–823 K) and from 3.5 to 7.7 nm in diameter.

It has been previously demonstrated by neutron and Raman scattering techniques<sup>17</sup> that compressive high pressure ( $>3$ –4 GPa) can also induce a shift in size dependence as represented schematically on the dotted line curve (Figure 4). But this compressive stress cannot explain the stabilization of MZ in our powders. The influence of a tensile stress was investigated based on thermodynamical considerations. For very small particles, the intragrain pressure  $P_{\text{int}}$  is different from external pressure  $P_{\text{ext}}$  due to the contribution of surface energy. The surface stress  $f$  induces a hydrostatic pressure  $\Delta p = f/2r$  on the interior of the particle where

$r$  is the particle radius and at the equilibrium,  $P_{\text{int}} = P_{\text{ext}} + 2\pi r$ . Therefore, the chemical potential  $\mu_{\varphi}^*(T, r)$  of a pure substance in the phase  $\varphi$  with spherical shape and finite size is given by the following relation,

$$\mu_{\varphi}^*(T, r) = \mu_{\varphi}^0(T) + \frac{3\gamma_{\varphi}\bar{V}_{\varphi}}{r} + P_{\text{ext}}\bar{V}_{\varphi} \quad (2)$$

in which  $\mu_{\varphi}^0(T)$ ,  $\gamma_{\varphi}$ , and  $\bar{V}_{\varphi}$  represent the standard chemical potential, the surface tension, and the molar volume of the phase  $\varphi$ , respectively.

The equilibrium  $(T_c, r_c)$  conditions are defined by the following equality:

$$\mu_{\text{MZ}}^*(T_c, r_c) = \mu_{\text{TZ}}^*(T_c, r_c) \quad (3)$$

Therefore, we can define a critical radius  $r_c$  for which both MZ and TZ coexist at a given temperature and external pressure by the relation

$$r_c = \frac{-3(\gamma_{\text{MZ}}\bar{V}_{\text{MZ}} - \gamma_{\text{TZ}}\bar{V}_{\text{TZ}})}{\mu_{\text{MZ}}^0 - \mu_{\text{TZ}}^0 + P_{\text{ext}}(\bar{V}_{\text{MZ}} - \bar{V}_{\text{TZ}})} \quad (4)$$

Let us define the parameter  $\eta$  as follows if we retain an isotropic surface energy:

$$1/\eta = 3(\gamma_{\text{MZ}}\bar{V}_{\text{MZ}} - \gamma_{\text{TZ}}\bar{V}_{\text{TZ}}) \quad \eta > 0 \quad (5)$$

Therefore, the temperature and pressure dependence of  $r_c$  can be rewritten for spherical particles in the general form

$$\frac{1}{r_c} = \eta[\Delta\mu^0(T) + \Delta\bar{V}P_{\text{ext}}] \quad (6)$$

with  $\Delta\mu^0$  and  $\Delta\bar{V}$  given for MZ and TZ by

$$\Delta\mu^0(T) = \mu_{\text{TZ}}^0 - \mu_{\text{MZ}}^0 \quad \Delta\mu^0(T) > 0 \text{ for } T < T_c(r_{\infty}) \quad (7)$$

$$\Delta\bar{V} = \bar{V}_{\text{TZ}} - \bar{V}_{\text{MZ}} \quad \Delta\bar{V} < 0 \quad (8)$$

The relation (6) underlines that the  $(T, P_{\text{ext}})$  evolution of  $r_c$  depends on the amplitude of the parameter  $\eta$  and the sign of the product  $\Delta\bar{V}$ . For zirconia, experimental values of  $\gamma_{\text{MZ}}$  and  $\gamma_{\text{TZ}}$  measured by Garvie are respectively equal to about 1.13 and 0.77  $\text{J}\cdot\text{m}^{-2}$ . The molar volume  $\bar{V}_{\text{TZ}}$  at room temperature was extrapolated by Chrsaka et al.<sup>5</sup> from neutron experiments at different temperatures;  $\bar{V}_{\text{MZ}}$  and  $\bar{V}_{\text{TZ}}$  are respectively equal to  $2.118 \times 10^{-5}$  and  $2.0225 \times 10^{-5} \text{ m}^{-3}$ . The term  $\Delta\bar{V}$  associated with the martensitic transition is negative in zirconia and high enough to induce a pressure effect from few GPa as shown in Figure 5.

The pressure-temperature phase diagram of zirconia proposed by Whitney<sup>18</sup> indicates that compressive stress decreases the temperature of transition MZ-TZ. Authors suggest that stress can be responsible for the stabilization of TZ at room temperature. Our calculations in the compressive stress domain correspond to the experimental values deduced from high-pressure observations made by neutron diffraction and Raman experiments. On the other hand, a tensile stress will induce the martensitic transition TZ  $\rightarrow$  MZ responsible

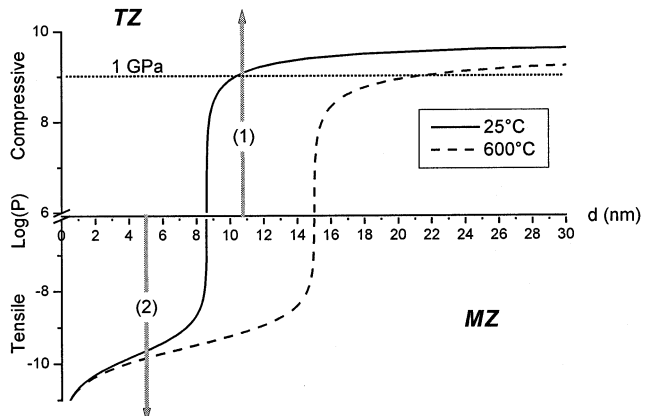


**Figure 5.** Calculated pressure-size stability domains of MZ and TZ deduced from eq 6 at room temperature (continuous line) and at 600 °C (dashed line).

for the transformation toughening mechanism used in sintered partially stabilized zirconia.

In our case, the relation (6) underlines that the spontaneous formation of ultrafine MZ particles at room temperature can be caused by two different mechanisms:

(1) A tensile stress at the particle surface induces a positive  $\Delta\bar{V}P_{\text{ext}}$  term, which increases the critical radius. However, this hypothesis is unlikely because experiments were made on free powder, after annealing at different temperatures up to 823 K, and under these conditions, the external surface stress is mainly relaxed. In stressed nanophase materials, the position, intensity, and peak width of Raman spectra are significantly different from those of the relaxed phase. However, the frequency of Raman lines observed in 3.6-nm zirconia obtained from room-temperature oxidation of ZrAu are similar to those of the relaxed bulk MZ.

(2) The parameter  $\eta$  was estimated to be equal to 34  $\text{kJ}\cdot\text{m}^{-3}\cdot\text{mol}^{-1}$  from experimental values of  $\gamma$  published by Garvie. However, the surface energy of finite size particles is strongly influenced by the presence of surface defects, adsorbed species, and the edge effects resulting from a faceted morphology. The surface tensions of the different  $(hk\bar{l})$  faces are strongly anisotropic and the average  $\bar{\gamma}$  for each particle is the result of the combination of the  $\gamma_{hk\bar{l}}$  and  $\gamma_{\text{defect}}$  contributions. Stabilization of MZ could be explained by a strong increase in the parameter  $\eta$ . Christensen and Carter<sup>19</sup> recently published theoretical results on the zirconia surface from first-principles calculations using density functional theory. They found that the surface tensions of the most stable faces of MZ and TZ (respectively  $(\bar{1}\bar{1}\bar{1})$  and  $(1\bar{1}\bar{1})$ ) are approximately equal (1.246 and 1.239  $\text{J}\cdot\text{m}^{-2}$ ). Under these conditions, the associated parameter  $\eta$  deduced from the theoretical values is much higher than those deduced from experimental data published for bulk zirconia. This would explain the stabilization of the monoclinic phase that we observed.

The major difference between TZ nanopowders previously studied and our MZ obtained from oxidation of ZrAu results from the conditions of preparation. Indeed, so far, zirconia nanopowders have been synthesized far from the equilibrium conditions, under relatively high

temperatures and in some cases under high pressure (for example, at near interface metal–oxide in pure zirconium corroded in high-pressure reactor use conditions<sup>20</sup>). As we show in Figure 5, the stability range of TZ increases drastically with  $P$  and  $T$ . After cooling, these particles are far from the equilibrium conditions and partially stabilized in the tetragonal (or cubic) phase. This stabilization is favored by an atomic organization similar to that of the initial amorphous zirconia. Nevertheless, according to the relation (6) and theoretical values of  $\gamma$ , a transformation into the more stable MZ occurs spontaneously after a long time, depending on defect concentration and adsorbed species.<sup>21–23</sup>

### Conclusion

This work has for the first time demonstrated that ultrafine monoclinic zirconia powder can be synthesized by spontaneous oxidation of ZrAu. Particle growth is limited to about 3.6 nm by the low-temperature process.

(20) Godlewski, J.; Bouvier, P.; Lucaleau, G.; Lafayette, L. *Zirconium in nuclear chemistry*, 12th International Symposium, Toronto, 1998.

(21) Ali, A. A. M.; Zaki, M. I. *Thermochim. Acta* **2002**, *387*, 29.

(22) Kim, Y. S.; Kwon, S. C. *J. Nucl. Mater.* **1999**, *270*, 165.

(23) Djurado, E.; Dessemond, L.; Roux, C. *Solid State Ionics* **2000**, *136–137*, 1249.

Thermodynamical calculations of  $T_c$  involving size effects underlined the role of surface energy and volume expansion upon martensitic transformation. MZ is the “true” stable phase at room temperature for both bulk and nanocrystals. The apparent contradiction with TZ formation generally observed could be explained by the nonequilibrium conditions used to produce these powders. Our results showed that the monotonic decrease of  $T_c$  for the martensitic transformation must be carefully considered. In the derived Gibbs–Thomson relation, the difference of  $\gamma$  is considered as the driving parameter for the size dependence of  $T_c$ . However, this difference is strongly modified in nanocrystals by surface and edge defects and anisotropic values of  $\gamma_{hkl}$ . The terms  $\eta$  and  $\Delta \bar{V}$  must be introduced to define the phase stability as a function of temperature, pressure, and particle size. Under these conditions, our experimental results confirm the theoretical calculations, which predicted equivalent surface energies for MZ and TZ.

**Acknowledgment.** The authors would like to thank M. Lomello-Tafin for preparation of starting ZrAu samples, professor G. Lucaleau and N. Rosman for their helpful contribution in Raman experiments, and professors J. L. Baudour and J. C. Niepce for valuable discussions.

CM021233N